Temperature-Induced Conformational Transition of a Model Elastin-like Peptide GVG(VPGVG)$_3$ in Water

Aliaksei Krukau, Ivan Brovchenko,* and Alfons Geiger

Physical Chemistry, University of Dortmund, Dortmund D-44221, Germany

Received February 26, 2007; Revised Manuscript Received April 25, 2007

The conformation of a single elastin-like peptide GVG(VPGVG)$_3$ in liquid water is studied by computer simulations in the temperature interval between 280 and 440 K. Two main conformational states of the peptide can be distinguished: a rigid conformational state, dominating at low temperatures, and a flexible conformational state, dominating at high temperatures. A temperature-induced transition between these states occurs at about 310 K, rather close to a transition temperature seen in experiments. This transition is accompanied by the thermal breaking of the hydrogen-bonded spanning network of the hydration water via a percolation transition upon heating. This finding indicates that the H-bond clustering structure of the hydration water plays an important role in the conformational stability of biomolecules. A second important observation is the Gaussian distribution of the end-to-end distance in the high-temperature state, which supports the idea of a rubber-like elasticity of the studied elastin-like peptide. Finally our results challenge the idea of the folding of elastin-like peptides upon heating.

Introduction

The ability of hydrated elastin to contract reversibly after stretching may be explained in the framework of the classical theory of rubber elasticity. In accordance with this theory, a chain with Gaussian (random) distribution of the end-to-end distance should show an elastic behavior.[1,2] Deviation from this distribution causes a decrease of entropy and the appearance of a restoring elastic force. This suggests studying the distribution of the end-to-end distance of elastin-like peptides (ELPs). For disordered, random coil conformations, this distribution should be Gaussian. Some experiments support this random coil model interpretation and evidence an isotropic structure,[3] conformational disorder,[4,5] and high mobility[6−8] of ELPs. Spectroscopic studies[9−11] demonstrate conformational heterogeneity of ELPs in liquid water, which is reflected in the simultaneous presence of various structural elements (α-helices, β-sheets, β-turns, γ-loops, and polyproline II and disordered structures). The relative population of these structures changes with temperature.[10−12] In particular, a minimum in the circular dichroism spectrum at 195 nm, which originates from a disordered structure and/or from polyproline II structures, becomes less pronounced with increasing temperature. Such a behavior was attributed to the increase of "order" in the structure of a single ELP upon heating.[10−15] The nature and degree of this "order" remain unclear. Of course, the elasticity of a highly ordered polypeptide chain cannot be explained, based on the entropic elasticity of a random chain, and requires another model of elasticity.[13−16] Thus, the physical origin of the elastic properties of the hydrated elastin is still a matter of debate.

Aqueous solutions of large ELPs exhibit a lower critical solution temperature (LCST), i.e., they undergo a first-order phase transition upon heating at some temperature T_t, that results in the separation of the solution into an organic-rich and a water-rich phase.[13−15] The temperature of this phase transition depends on the amino acid composition of the ELP, its concentration, addition of cosolvents, pH, etc. Similar to other polymers, whose aqueous solutions show a LCST,[17−19] ELPs drastically change their conformational distribution when crossing T_t.[10−15] A macroscopic phase separation of the aqueous solutions of small ELPs (from one to several pentameric VPGVG units)[10,11,20] into organic-rich and water-rich phases upon heating was not detected. Their conformational changes are qualitatively similar to those detected for large ELPs, when crossing T_t, but are observed in a wider temperature interval.[10,11]

Understanding the microscopic origin of the temperature-induced conformational transition of the ELPs, as well as characterizing their conformations below and above T_t by computer simulation studies, should help to clarify the mechanism of their elasticity. In particular, such studies should show whether an ELP exhibits a random distribution of the end-to-end distance or whether its structure is more ordered. As a phase separation of the aqueous solutions of ELPs may be expected, ideally such systems should be studied by appropriate simulation methods (such as simulations in the grand canonical or Gibbs ensemble, etc.). These methods imply the necessity to insert randomly solute molecules in a rather dense liquid phase, and therefore their applicability strongly diminishes with increasing solute size. As a result, now and in the near future, phase transitions in aqueous solutions even of small biomolecules cannot be studied by direct simulation methods. In such a situation, studies of a *single* biomolecule in liquid water remain the most popular simulation approach. They give useful information concerning the properties of the biomolecule and the surrounding water at various thermodynamic conditions. However, when comparing computational results with experiments, the intrinsic inability of *single* biomolecule simulation to reproduce the phase transition of a solution should be taken into account.

The most detailed simulation studies of the temperature-induced conformational changes of a single ELP in water were performed for a small elongated pentapeptide GVG(VPGVG)[20,21] and a polypentapeptide (VPGVG)$_{18}$.[22] Two main structures, compact and extended (with and without intramolecular hydrogen bonds, respectively) were found for the small GVG-(VPGVG) peptide. The extended structure dominates in the

* To whom correspondence should be addressed. E-mail: brov@heineken.chemie.uni-dortmund.de.

10.1021/bm070233j CCC: $37.00
Published on Web 06/14/2007

whole studied temperature range 280 to 380 K, the highest population of the compact structure occurs at about 330 K.[20,21] Most important, above this temperature, a peptide mode, which reflects a transition between the two main structures, noticeably speeds up. Interestingly, the temperature dependence of the dynamics of the water−peptide hydrogen bonds also qualitatively changes at about 330 K. The simulations of the much larger polypentapeptide $(VPGVG)_{18}$ did not reveal an ordered structure,[22] despite the fact that the simulations were started from a conformation, which corresponds to an ordered β-spiral. Already after a short equilibration, this ELP adopts an "amorphous" structure, which is more compact (and has more intramolecular H-bonds) at higher temperatures.

The simulation studies of single ELPs in water did not yet answer the key question, concerning the origin of the elastic properties of the ELPs: does a single ELP show a random distribution of the end-to-end distance in water? The GVG(VPGVG) peptide[21] is too small to show distributions, which are characteristic for long chains, whereas simulation runs of 10 to 20 ns[22] are obviously not long enough for an adequate sampling of the structure of the large polypentapeptide $(VPGVG)_{18}$ chain in water. To avoid these problems, we have simulated a polypentapeptide of intermediate size GVG$(VPGVG)_3$ in water during extremely long times (up to 350 ns). In this paper we present structural properties of this peptide as well as properties of the spanning hydrogen-bonded network of the hydration water at various temperatures.

Model System, Simulation, and Analysis Methods

Simulations of ELP in Water. A left handed β-spiral[13−15] was used as an initial conformation of the small ELP GVG$(VPGVG)_3$, capped by methylamine ($-NH-CH_3$) and acetyl ($-CO-CH_3$) at the C- and N-termini, respectively. The ELP was initially equilibrated in vacuum for 10 ps at 300 K and then placed in a cubic box with 1224 water molecules. Periodic boundary conditions were applied, and the system was equilibrated for 5 ns at 300 K. In the resulting conformation the β-spiral had disappeared. It was used as the initial one for all simulations of the ELP in liquid water at 12 temperatures between 280 and 440 K. Molecular dynamics (MD) simulations were performed in the *NPT* ensemble at constant pressure $P = 1$ bar, using the Nose−Hoover thermostat and the Parrinello−Rahman barostat. The Gromacs software package[23] was used with the all-atom AMBER94 force field[24] for the ELP molecule and the SPCE model[25] for water. A spherical cutoff of 9 Å was used for the short-range intermolecular interactions; the long-range Coulombic interactions were taken into account by particle mesh Ewald summation. All simulation runs were performed with 2 fs time steps for 350 ns at $T = 280$, 300, 320, 340, 360, and 380 K, for 180 ns at $T = 285$, 290, and 295 K, and for 120 ns at $T = 400$, 420, and 440 K. Molecular configurations were analyzed every 2 ps; the first 5 ns were discarded from the analysis. A total of 6×10^4 to 1.7×10^5 configurations were analyzed for each temperature.

Conformational Analysis of ELP. The end-to-end distance R, the radius of gyration S, and the maximal extension L of the ELP were used to characterize its conformation. R is equal to the distance between the methyl carbon atoms of the end groups. S was calculated taking into account the positions of all heavy atoms of the ELP. The average values of R, S, and L as well as their probability distributions $P(R)$, $P(S)$, and $P(L)$ were calculated for each temperature. The probability distributions were fitted by the equation

$$P(A) \sim (A - A_0)^{\alpha} \exp(-B_A(A - A_0)^{\beta}) \qquad (1)$$

where A denotes R, S, or L; A_0, B_A, α, and β are fitting parameters. The pre-exponential factor reflects the increase of the configurational space with R, S, and L. For a Gaussian (random) chain $\alpha = \beta = 2$ in the distribution $P(R)$.[26] To analyze the temperature-induced conformational changes of the ELP, the parameters obtained from the fit as well as the quality of the fits were derived as a function of temperature. The probability distribution of the end-to-end distance $P(R)$ was also fitted to the equation for a semiflexible, worm-like chain:[27]

$$P(R) \sim (R - R_0)^{\alpha}(\exp(-B_R(R - R_0)^{\beta}))(1 + C_R(R - R_0)^{\gamma}) \qquad (2)$$

which contains one more fitting parameter (C_R) in comparison with eq 1.

Ramachandran diagrams,[28] which represent correlations between the dihedral angles φ and ψ of the amino acid residues in the peptide structure, were used to analyze the presence of specific structural elements in the ELP conformation. Two characteristic regions of the Ramachandran plot (within $-90° < \varphi < -35°$, $-70° < \psi < -15°$ and within $-105° < \varphi < -45°$, $120° < \psi < 180°$) were attributed to α-helix and to polyproline II structures, respectively. To get information about the distribution of these structural elements along the peptide chain, we have calculated distributions n_m of the probability to find exactly m successive residues with the same structure. Such an analysis was performed separately for the α-helix and for the polyproline II structural elements.

Additionally, we analyzed the temperature dependence of the intramolecular peptide−peptide H-bonds between the i-th and $(i + \Delta i)$-th residues. Two residues were considered as H-bonded, when the distance between their oxygen and nitrogen atoms does not exceed 3.5 Å and the angle NHO is above 130°. H-bonds with $2 \le \Delta i \le 5$ correspond to some ordered structural elements, whereas H-bonds with $\Delta i > 5$ are attributed to some less ordered structures.

Percolation Analysis of Hydration Water. The state of the hydrogen-bonded (HB) water network in the hydration shell of ELP at various temperatures was characterized by an analysis of the water clustering. A water molecule was considered as belonging to the hydration shell, when the shortest distance between its oxygen and the heavy atoms of ELP does not exceed 4.5 Å. This criterion is based on the water density distribution near the surface of biomolecules.[29] The existence of an H-bond between two water molecules is used as a connectivity criterion. Two molecules were considered as H-bonded; when the distance between their oxygens did not exceed 3.35 Å and their pair interaction energy was below −2.7 kcal/mol. These criteria yield about 3.3 H-bonds per water molecule on average in pure liquid water at ambient conditions. The analysis of the water clustering and percolation in the hydration shell was performed similarly to our previous studies of the percolation transition of water in aqueous systems.[28−31] The distribution of the size of the largest HB water cluster in the hydration shell was used to estimate the probability SP (spanning probability) to find a water cluster, which homogeneously envelopes the ELP (see refs 29−32 for more details). The structure and spanning character of the largest cluster of hydration water was characterized by its radius of gyration S_w, maximal extension L_w, and by the distance H_w between its center of mass and the center of mass of the ELP.

Results

The fluctuation of the maximal extension L of ELP at various temperatures is shown in Figure 1. At $T = 280$ K two different conformational states of ELP can be distinguished (see upper panel of Figure 1). In the time interval from 80 to 180 ns, the average value $L^{av} = 20.40 \pm 0.80$ Å, and in the time interval from 200 to 300 ns, $L^{av} = 22.76 \pm 2.32$ Å. Because of the smaller fluctuation of L, in the first conformational state the ELP can be considered to be more *rigid*, whereas in the second state it is more *flexible* and slightly more extended. The transitions between these two states are reversible. The fraction of the rigid conformational state of ELP quickly decreases with

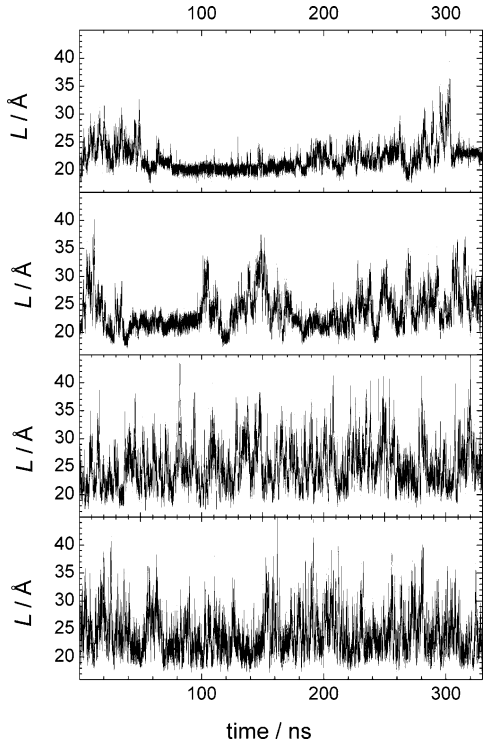

Figure 1. Variation of the maximal extension L of the ELP with time at various temperatures. From top to bottom: $T = 280$, 300, 340, and 380 K.

increasing temperature. The presence of this state may be noticed at $T = 280-320$ K, but at $T = 340$ K and higher temperatures only the flexible conformational state of ELP is seen in the time dependence of L (Figure 1).

The time dependences of the other structural characteristics of the ELP, such as the end-to-end distance R and the radius of gyration S, are qualitatively similar to the time dependence of L, shown in Figure 1. The correlations between R, S, and L at low temperature (rigid state dominates) and at high temperature (flexible state dominates) are shown in the two lower panels of Figure 2. At $T = 280$ K, the average values $R^{av} = 13.03 \pm 1.83$ Å and $S^{av} = 6.19 \pm 0.18$ Å in the time interval from 80 to 180 ns (rigid state), whereas in the time interval from 200 to 300 ns (flexible state) $R^{av} = 13.73 \pm 4.34$ Å and $S^{av} = 6.82 \pm 0.66$ Å. The number N_w of water molecules in the hydration shell of the ELP (proportional to the solvent accessible surface area at constant temperature) also clearly correlates with L. Similar to other structural characteristics of the ELP, N_w fluctuates slightly at $T = 280$ K and in a much wider range at $T = 440$ K. Due to the decrease of the liquid water density with temperature, the average value of N_w also decreases (see Figure 2).

The properties of the hydrogen-bonded network of the hydration water at the surface of the ELP are quite different at low and high temperatures. At $T = 280$ K, the center of mass of the largest HB cluster of hydration water is very close to the center of mass of the ELP, and the distance H_w between these two centers is close to zero (see left panel in Figure 2). This clearly indicates the presence of a spanning HB water network, which *homogeneously* envelopes ELP at all extensions L. In contrast, at high temperatures (right panel in Figure 2) the value of H_w is high and varies in a wide range without any correlation with L. Another parameter of the hydration water network, the maximal extension L_w of the largest water cluster, shows a clear correlation with the maximal extension L of the ELP at low temperatures, whereas at high temperatures such a correlation

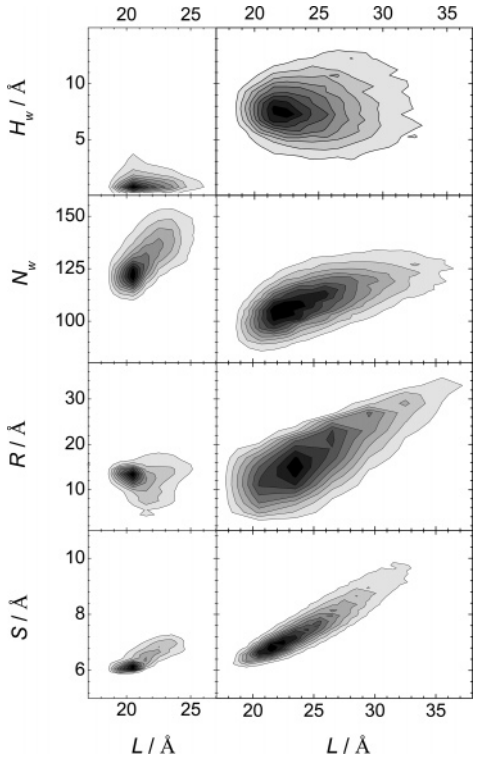

Figure 2. Correlations between the maximal extension (L) of the ELP and (from bottom to top) its radius of gyration (S), end-to-end distance (R), number of water molecules in the hydration shell of the ELP (N_w), and distance between the centers of mass of the ELP and of the largest water cluster in the hydration shell (H_w). Left panel: $T = 280$ K (rigid conformational state of ELP dominates). Right panel: $T = 440$ K (flexible conformational state of ELP dominates).

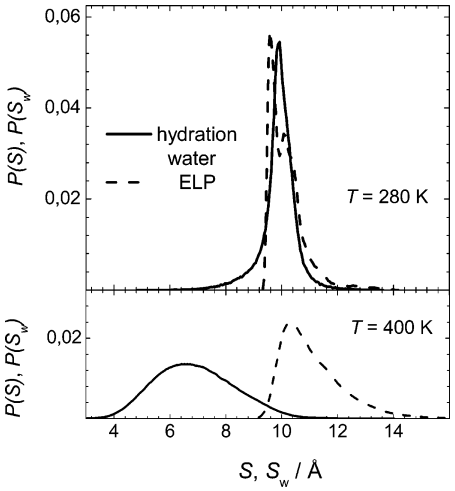

Figure 3. Probability distributions of the radius of gyration (S) of the ELP and of the radius of gyration (S_w) of the largest hydrogen-bonded cluster in the hydration shell of ELP at two different temperatures. (The ELP distribution is shifted by +3.5 Å at both temperatures.)

is practically absent (not shown). The radius of gyration S_w of the largest water cluster in the hydration shell of the ELP at low temperatures (see distribution in the upper panel of Figure 3) exceeds the radius of gyration S of the ELP by about 3.5 A (about the width of a water layer), indicating homogeneous coverage of the ELP by the spanning HB water network. The strong difference of S and S_w at higher temperatures (see lower panel of Figure 3) indicates the absence of a spanning network of hydration water. The temperature dependence of the average value S^{av} of the radius of gyration of the ELP (Figure 4, upper panel) shows two characteristic temperature intervals: the

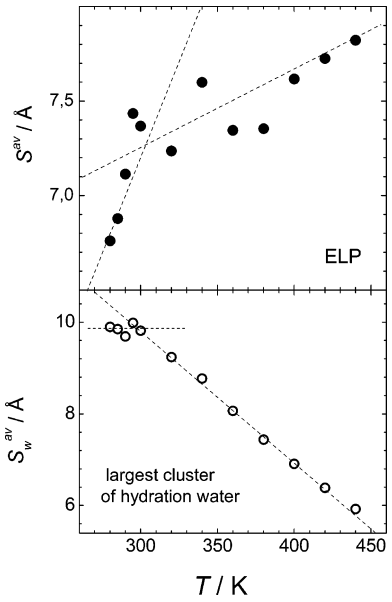

Figure 4. Average radius of gyration (S^{av}) of ELP (upper panel) and average radius of gyration (S_w^{av}) of the largest hydrogen-bonded cluster in the hydration shell of ELP (lower panel).

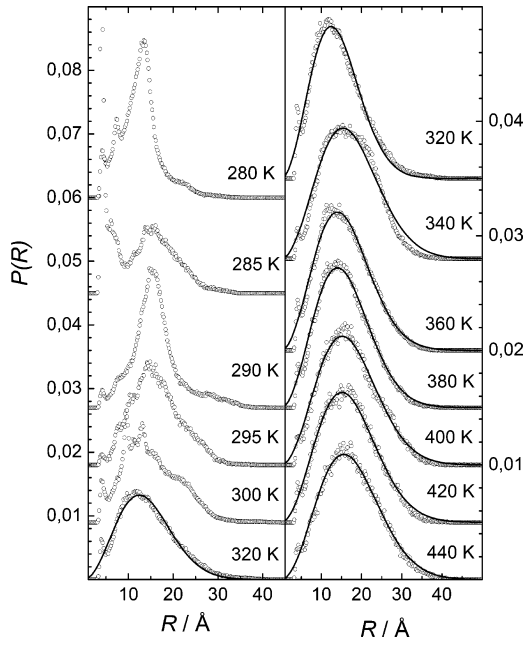

Figure 5. Probability distributions ($P(R)$) of the end-to-end distance (R) of the ELP at various temperatures (circles) and the fits using eq 1 with $\alpha = 2$ and $\beta = 2$ (lines). To separate the different distributions they are shifted vertically. Note also the different scales for the left and right panel.

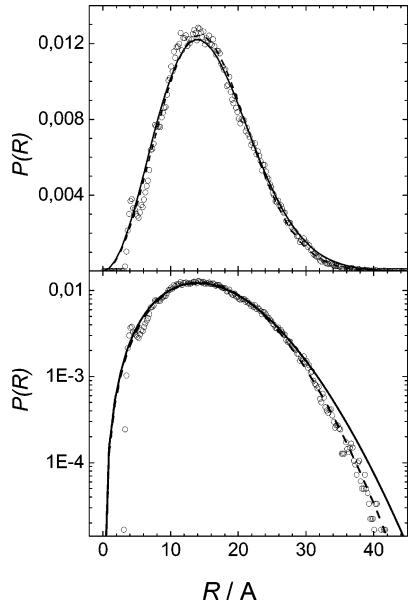

Figure 6. Probability distributions ($P(R)$) of the end-to-end distance (R) of ELP at $T = 380$ K (circles) and the fits to the distribution of the random chain (eq 1 with $\alpha = 2$ and $\beta = 2$, solid lines) and to the distribution of the worm-like chain (eq 2, dashed lines). Lower panel: logarithmic scale.

increase of S^{av} is stronger at $T < 310$ K and weaker at $T > 310$ K. This indicates a qualitative change of the conformational state of the ELP at $T \approx 310$ K, which should be attributed to the lower occupation of the rigid conformational state with increasing temperature. Interestingly, the average radius of gyration S_w^{av} of the HB network of hydration water also shows two quite different temperature dependences: below about 300 K, S_w^{av} practically does not depend on temperature, whereas at higher temperatures it almost linearly decreases with T (see lower panel of Figure 4).

To clarify the difference between the rigid and the flexible conformational states of the ELP, we have analyzed the shape of the probability distributions $P(R)$, $P(S)$, and $P(L)$ at various temperatures (see circles in Figures 5−8). Fitting of eq 1 to the probability distribution $P(R)$ of the end-to-end distance R of ELP gives values of the fitting parameters α and β, which vary with temperature. In the temperature interval from 320 to 440 K, both α and β have the closest integral value 2, whereas at lower temperatures they strongly deviate from this value. The fitting parameter R_0 was close to zero in all cases. Subsequently, we have fitted eq 1 to the distributions $P(R)$ keeping $\alpha = \beta = 2$ and $R_0 = 0$ (see lines in Figure 5), which corresponds to the distribution of the end-to-end distance for a Gaussian (random) chain. The fitting curves quite satisfactorily reproduce the distributions $P(R)$ at $T \geq 320$ K. In Figure 6 the distribution $P(R)$ and the fit to eq 1 with $\alpha = \beta = 2$ at $T = 380$ K are shown in a logarithmic scale. A systematic deviation of the fit from $P(R)$ may be noticed at $R > 30$ Å only. This deviation is strongly diminished when eq 2 is used to fit $P(R)$. This equation describes the distribution of the end-to-end distance for a worm-like chain (see lower panel in Figure 6). Note, however, that the presence of one more fitting parameter in eq 2 in comparison with eq 1 improves the fit only for large values of R, which the ELP exhibits rather rarely. This is in agreement with atomic force microscopy stretching experiments on single polymer chains, which show at large extensions a better agreement with worm-like chain behavior.[33]

The analysis of the probability distributions $P(S)$ and $P(L)$ of the radius of gyration S of the ELP and of its maximal extension L was performed in a similar way. Fitting of eq 1 to the probability distribution $P(S)$ gives the closest integral value 1 for the parameters α and β in the temperature interval from 320 to 440 K. Thus, we have fitted the distributions $P(S)$ with eq 1 keeping $\alpha = \beta = 1$ and $S_0 = 6.05$ Å (the average value of S_0 at 320 K $\leq T \leq$ 440 K). In the temperature interval from 320 to 440 K, fitting of the probability distribution $P(L)$ with eq 1 gives the closest integral value 2 for the parameter α and 1 for the parameter β. Consequently, we have fitted the distributions $P(L)$ with eq 1 keeping $\alpha = 2$, $\beta = 1$, and $L_0 = 17.72$ Å (the average value of L at 320 K $\leq T \leq$ 440 K). The probability distributions $P(S)$ and $P(L)$ and their fits using eq 1 are shown in Figures 7 and 8, respectively. The fitting curves (lines in Figures 7 and 8) reproduce well the obtained distribu-

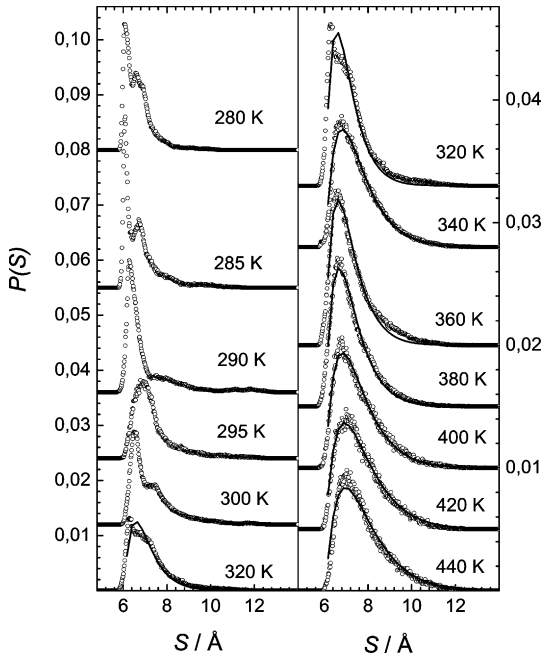

Figure 7. Probability distribution ($P(S)$) of the radius of gyration (S) of ELP at various temperatures (circles) and fits using eq 1 with $\alpha = 1$ and $\beta = 1$ (lines). The different distributions are shifted vertically to avoid overlapping.

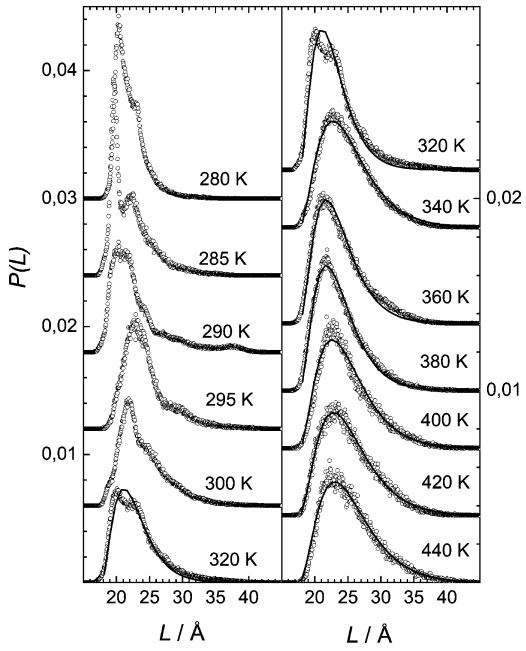

Figure 8. Probability distribution ($P(L)$) of the largest distance between two atoms (L) of ELP at various temperatures (circles) and fits using eq 1 with $\alpha = 2$ and $\beta = 1$ (lines). The different distributions are shifted vertically to avoid overlapping.

tions at $T \geq 320$ K, whereas at lower temperatures it is not possible, as the distributions $P(S)$ and $P(L)$ show multiple peaks.

The ability of eqs 1 and 2 to describe the probability distributions $P(R)$, $P(S)$, and $P(L)$ drastically worsens below 320 K. The quality of the fits was characterized by the ratio $\Delta P(A) = \chi_A^2(T)/\chi_A^2(440\text{ K})$ of two variances $\chi_A^2 = \langle (P(A) - P(A)^{\text{fit}})^2 \rangle$, which measure the deviation of the obtained distribution $P(A)$ from the fitting function $P(A)^{\text{fit}}$ at a given temperature, and A denotes R, S, or L. The temperature dependences of $\Delta P(R)$, $\Delta P(S)$, and $\Delta P(L)$ are shown in the middle panel of Figure 9. Obviously, the ability of eq 1 to describe adequately the shape of the distribution $P(A)$ is almost independent of T in the interval

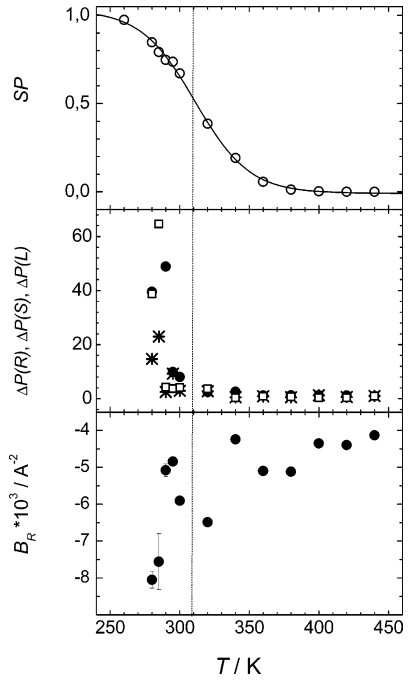

Figure 9. Existence probability (SP) of a spanning network in the hydration shell of the ELP (upper panel). Deviations $\Delta P(R)$ (circles), $\Delta P(S)$ (squares), and $\Delta P(L)$ (stars) of the probability distributions $P(R)$, $P(S)$, and $P(L)$ from the fits to eq 1 (middle panel) are shown. Parameter B_R (full circles) values are obtained from the fits of eq 1 to $P(R)$ (lower panel). Vertical dashed line indicates the temperature where SP = 50%.

between 440 K and about 320 K, whereas at lower temperatures the shape of $P(A)$ changes drastically and, in particular, for $P(R)$ it strongly deviates from the distribution of the end-to-end distance for the random chain. The temperature dependence of the fitting parameter B_R is shown in the bottom panel of Figure 9. This value varies only slightly with temperature at $T \geq 340$ K and decreases at low temperatures, indicating a growing fraction of the more rigid conformational state of ELP.

Thus, the analysis of the shapes of the probability distributions $P(R)$, $P(S)$, and $P(L)$ at various temperatures evidences a temperature-induced conformational transition of ELP at $T_t \approx 310$ K. In conjunction with the observed fluctuations (Figure 1), we may conclude that, at $T > T_t$, the ELP is a flexible chain with random distribution of the end-to-end distance, whereas the residence time in a more rigid conformational state quickly grows upon cooling below T_t. Interestingly, the appearance of a more rigid state of the ELP is accompanied by the formation of a spanning HB water network around the ELP. In other words, the H-bond-enveloped conformation is more rigid, whereas the disappearance of the strongly connected H-bond network promotes higher flexibility of the peptide. The evolution of the spanning network of hydration water can be seen from the temperature dependence of the existence probability SP (see Percolation Analysis section) shown in the upper panel of Figure 9.

The content of α-helix and polyproline II structural elements can be obtained from the distributions of the dihedral angles φ and ψ of the amino acid residues. The temperature dependence of this quantity is shown in the upper panel of Figure 10. At low temperatures, the content of both structures is comparable. Upon heating up to T_t, the content of polyproline II structures decreases, which is in agreement with experimental CD studies,[10−12] whereas the content of α-helices increases. At higher temperatures, these occurrence frequencies vary but do not show some clear trends. The presence of ordered structural

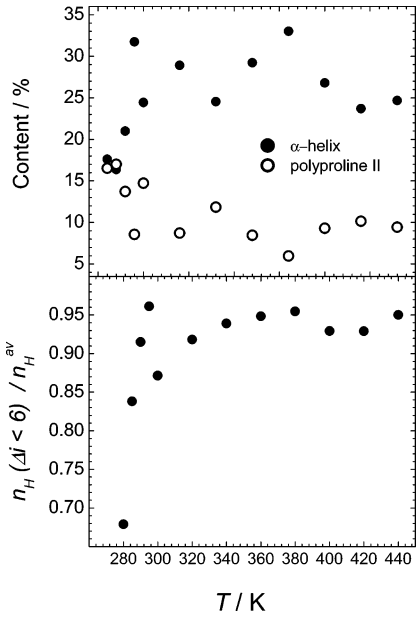

Figure 10. Temperature dependence of the content of α-helix and polyproline II structures (upper panel), and temperature dependence of the fraction of intramolecular H-bonds between the *i*-th and ($i + \Delta i$)th residues with $\Delta i < 6$ (lower panel).

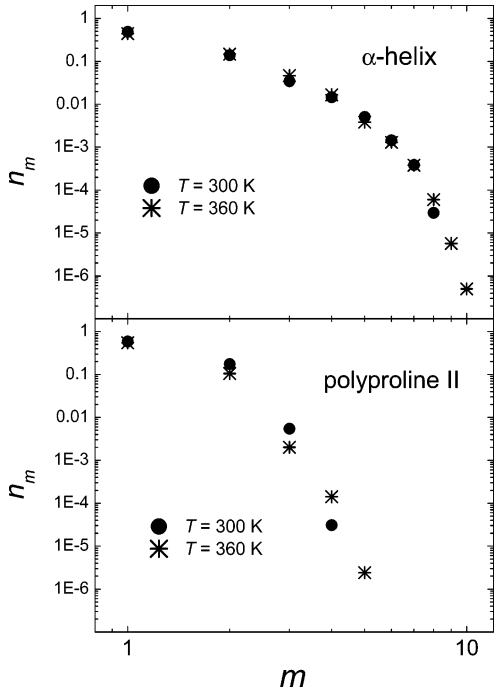

Figure 11. Distribution of the probability (n_m) to find *m* successive residues with the same structure.

elements in the peptide chain can be indicated by the intramolecular H-bonds between the *i*-th and ($i + \Delta i$)th residues, with $2 \leq \Delta i \leq 5$. The temperature dependence of the number of such H-bonds, normalized by the average number n_H^{av} of intramolecular H-bonds, is shown in the lower panel of Figure 10. At $T > T_t$, the occurrence of ordered structural elements does not change noticeably with temperature. At lower temperatures, their population drastically decreases, indicating the appearance of some irregular intramolecular H-bonds with $\Delta i > 5$.

Distributions n_m of the probability to find *m* successive residues with the same structure are shown in Figure 11. At all temperatures studied, about 40 to 60% of the residues with the certain structure have no neighbors with the same structure ($m = 1$). About 20 to 30% of all residues with the same structure form pairs ($m = 2$). The probability to find *m* successive residues with the same structure drastically decreases with increasing *m* in a strictly monotonic way. This indicates an essentially random distribution of the residues with α-helix or polyproline II structures along the peptide chain.

Discussion

Two quite different conformational states of the model ELP GVG(VPGVG)$_3$ are seen in the simulations. At high temperatures, the ELP is a highly flexible chain, which shows a random distribution of the end-to-end distance. Moreover, the parameter B_R in the exponent of eq 1 does not vary strongly with temperature, at least at $T \geq 340$ K (see lower panel of Figure 9). This finding evidences the mainly entropic character of the elasticity of the ELP and supports an old idea of Hoeve and Flory that the elasticity of elastin is rubber-like.[1,2] The random distribution of the end-to-end distances of the high-temperature conformational states of the ELP suggests a random coil structure. But, the presence of various structural elements (see Figure 10) and the essential number n_H^{av} of intramolecular H-bonds (in the considered temperature range, n_H^{av} varies from about 5.5 to 6.5) seem to contradict this conclusion. However, an irregular (or even random) location of the ordered structural elements along the chain (see Figure 11) and/or a frequent interconversion between them may well provide a random distribution of the end-to-end distance of a chain. In general, an interconversion between the various structural elements of the chain is accompanied by a rearrangement of the intramolecular H-bonds. Obviously, the presence of hydration water, which is a plasticizer for biomolecules, should strongly facilitate this rearrangement. This may explain why only hydrated ELPs show elastic properties.[34]

The observed flexible conformational state of the ELP combines the presence of local order with a random (disordered) character of the full peptide chain. This picture is supported by the isotropic structure[3] and high mobility[6] of ELPs, seen in experiments. The presence of the ordered structural elements in ELPs is clearly seen both in experiment[9−11] and in simulations (see ref 22 and Figure 10). However, there is no evidence that these structures are distributed along the chain nonrandomly. When the simulation starts from a highly ordered conformational state of the ELP (for example, a β-spiral[13−15] was used as initial state of the ELP in ref 22 and in our studies), it vanishes quickly and the ELP becomes a disordered ("amorphous"[22]) chain. Finally, in our simulation studies, we have found essentially random distribution of the ordered structural elements along the peptide chain (Figure 11).

Below $T_t \approx 310$ K another, more rigid, conformational state of the ELP, which does not show a random distribution of the end-to-end distance, appears, and its fraction drastically increases upon cooling. The low-temperature rigid state differs from the high-temperature flexible conformational state of the ELP by the presence of an irregular pattern of intramolecular H-bonds between amino acids that are separated by more than 5 residues (see lower panel of Figure 10). The number of such intramolecular H-bonds drastically decreases upon heating above $T_t \approx 310$ K. When crossing T_t, the state of the hydration water shell also changes drastically: below T_t, most of the water molecules in the hydration shell of the ELP form a spanning network of HBs; above T_t, the hydration water decomposes into small HB clusters.[29] The thermal breaking of the spanning network of the

hydration water upon heating occurs via a quasi-2D percolation transition at about T_t and may be considered as a transition of the hydration water from a more ordered state (large spanning network) to a less ordered state (ensemble of small clusters). This qualitative change of the hydration water state may be responsible for the appearance of a flexible conformational state above T_t: contrary to the spanning water network, small water clusters in the hydration shell may not hamper interconversions between various local structures of the ELP, which seem to be important for the flexibility of the ELP chain.

Clearly, the rigid low-temperature conformational state of the ELP, seen in our simulations, does not resemble a random coil, as it does not show a random distribution of the end-to-end distance. This contradicts the idea that the ELP is a random coil at low temperatures.[10,13−15] This idea has been based mainly on the specific temperature behavior of a minimum in the CD spectrum of the ELP in water at 195 nm: it becomes less negative with increasing temperature.[10−12] This minimum was attributed to the random coil state of the ELP, and its disappearance upon heating was therefore attributed to the increasing order of the ELP chain. Moreover, this interpretation of the CD spectra gave rise to the idea that ELPs, in contrast to most other biomolecules, undergo a folding upon heating ("inverse temperature transition").[13−15] When we consider an aqueous solution of the ELP, an increase of order at macroscopic level upon heating appears as it separates into two phases at LCST. Of course, this decrease of entropy at the macroscopic level is overcompensated by its increase at the microscopic level upon heating[35] (breaking of intra- or intermolecular H-bonds, disordering of hydration water, etc.). However, a *single* ELP chain does not necessarily become more ordered upon heating. The minimum of CD spectra at 195 nm is attributed not only to a random coil but also to an ordered polyproline II structure.[36−39] This structure disappears upon thermal denaturation of some proteins.[40] This causes a change of the CD spectra which is qualitatively very similar to the one observed upon "inverse temperature transition" of ELP. Moreover, the minimum at 195 nm in the CD spectra of ELPs in water is much less negative at low temperatures than one would expect for a random coil.[8] Our simulation results also indicate a decrease of the content of the polyproline II structures upon heating (see upper panel in Figure 10). Thus the results both of experiments and simulations can be explained without the assumption of folding of the ELPs upon heating. The conformational transition of hydrated ELPs upon heating appears rather as a redistribution of the populations of the various locally ordered structures. The main redistribution seems to be connected with a decrease of polyproline II structures and the appearance of other structures such as β-turns, γ-loops, etc.[10−12] Interestingly, it was observed that the hydration water network stabilizes polyproline II structures.[36] This may explain why the thermal breaking of the spanning network of hydration water and the conformational transition of ELP occur simultaneously.

Acknowledgment. We thank DFG Forschergruppe 436 for financial support.

References and Notes

(1) Hoeve, C. A. J.; Flory, P. J. *J. Am. Chem. Soc.* **1958**, *80*, 6523−6526.
(2) Hoeve, C. A. J.; Flory, P. J. *Biopolymers* **1974**, *13*, 677−686.
(3) Aaron, B. B.; Gosline, J. M. *Nature* **1980**, *287*, 865−867.
(4) Yao, X. L.; Hong, M. *J. Am. Chem. Soc.* **2004**, *126*, 4199−4210.
(5) Pometun, M.; Chekmenev, E.; Wittebort, R. *J. Biol. Chem.* **2004**, *279*, 7982−7987.
(6) Torchia, D. A.; Piez, K. A. *J. Mol. Biol.* **1973**, *76*, 419−424.
(7) Bochicchi, B.; Floquet, N.; Pepe, A.; Alix, A. J. P.; Tamburro, A. *Chem.−Eur. J.* **2004**, *10*, 3166−3176.
(8) Debelle, L.; Alix, A. J. P. *Biochimie* **1999**, *81*, 981−994.
(9) Debelle, L.; Alix, A. J. P.; Wei, S. M.; Jacob, M. P.; Huevenne, J. P.; Berjot, M.; Legrand, P. *Eur. J. Biochem.* **1998**, *258*, 533−539.
(10) Reiersen, H.; Clarke, A. R.; Rees, A. R. *J. Mol. Biol.* **1998**, *283*, 255−264.
(11) Nicolini, C.; Ravindra, R.; Ludolph, B.; Winter, R. *Biophys. J.* **2004**, *86*, 1385−1392.
(12) Urry, D. W.; Trapane, T. L.; Prasad, K. U. *Biopolymers* **1985**, *24*, 2345−2356.
(13) Urry, D. W. *J. Phys. Chem. B* **1997**, *101*, 11007−11028.
(14) Urry, D. W.; Parker, T. M. *J. Muscle Res. Cell Motil.* **2002**, *23*, 543−559.
(15) Urry, D. W.; Hugel, T.; Seitz, M.; Gaub, H. E.; Sheiba; L.; Dea, J.; Xu, J.; Parker, T. *Philos. Trans. R. Soc. London, Ser. B* **2002**, *357*, 169−184.
(16) Li, B,; Daggett, V. *J. Muscle Res. Cell Motil.* **2002**, *23*, 561−573.
(17) Winnik, F. M. *Macromolecules* **1990**, *23*, 233−242.
(18) Luna-Barcenas, G; Meredith, J. C.; Sanchez, I. C.; Johnston, K. P. *J. Chem. Phys.* **1997**, *107*, 10782−10792.
(19) Maeda, Y.; Nakamura, T.; Ikeda, I. *Macromolecules* **2001**, *34*, 1391−1399.
(20) Schreiner, E.; Nicolini, C.; Ludolph, B.; Ravindra, R.; Otte, N.; Kohlmeyer, A.; Rousseau, R.; Winter, R.; Marx, D. *Phys. Rev. Lett.* **2004**, *92*, 148101−4.
(21) Rousseau, R.; Schreiner, E.; Kohlmeyer, A.; Marx, D. *Biophys. J.* **2004**, *86*, 1393−1407.
(22) Li, B.; Alonso, O. V. D.; Daggett, V. *J. Mol. Biol.* **2001**, *305*, 581−592.
(23) Lindahl, E.; Hess, B.; van der Spoel, D. *J. Mol. Model.* **2001**, *7*, 306−317.
(24) Cornell, W. D.; Cieplak, P.; Bayly, C. I.; Gould, I. R.; Merz, K. M.; Ferguson, D. M.; Spellmeyer, D. C.; Fox, T.; Caldwell, J. W.; Kollman, P. A. *J. Am. Chem. Soc.* **1995**, *117*, 5179−5197.
(25) Berendsen, H. J. C.; Grigera, J. R.; Straatsma, T. P. *J. Phys. Chem.* **1987**, *91*, 6269−6271.
(26) Flory, P. J. *Principles of Polymer Chemistry*; Cornell University Press: Ithaca, New York, 1953.
(27) Yamakawa, H. *Modern Theory of Polymer Solutions*; Harper & Row Publishers: New York, 1971.
(28) Ramachandran, G. N.; Ramakrishnan, C.; Sasisekharan, V. *J. Mol. Biol.* **1963**, *7*, 95−99.
(29) Brovchenko, I.; Krukau, A.; Smolin, N.; Oleinikova, A.; Geiger, A.; Winter, R. *J. Chem. Phys.* **2005**, *123*, 224905−10.
(30) Oleinikova, A.; Smolin, N.; Brovchenko, I.; Geiger, A.; Winter, R. *J. Phys. Chem. B* **2005**, *109*, 1988−1998.
(31) Smolin, N.; Oleinikova, A.; Brovchenko, I.; Geiger, A.; Winter, R. *J. Phys. Chem. B* **2005**, *109*, 10995−11005.
(32) Oleinikova, A.; Brovchenko, I.; Smolin, N.; Krukau, A.; Geiger, A.; Winter, R. *Phys. Rev. Lett.* **2005**, *95*, 247802−4.
(33) Nakajima, K.; Watabe, H.; Nishi, T. *Polymer* **2006**, *47*, 2505−2510.
(34) Kakivaya, S. R.; Hoeve, C. A. J. *Proc. Natl. Acad. Sci.* **1975**, *72*, 3505−3507.
(35) Hirschfelder, J.; Stevenson, D.; Eyring, H. *J. Chem. Phys.* **1937**, *5*, 896−912.
(36) Fatma, E.; Griebenov, K.; Schweitzer-Stenner, R. *J. Am. Chem. Soc.* **2003**, *125*, 8178−8185.
(37) Sreerama, N.; Woody, R. *Biochemistry* **1994**, *33*, 10022−10025.
(38) Gocke, I.; Woody, R.; Anderluh, G.; Lakey, J. H. *J. Am. Chem. Soc.* **2005**, *127*, 9700−9701.
(39) Sreerama, N.; Woody, R. *Protein Sci.* **2003**, *12*, 384−388.
(40) Wu, J.; Yang, J. T.; Wu, C.-S. C. *Anal. Biochem.* **1992**, *200*, 359−364.

BM070233J